HJHPD

HJ

Article

Co-Occurrence of Hidden Severe Malaria Burden and Zero-Dose Childhood Vulnerability Across Kano State, Nigeria

Yakubu Joel Cherima[1], Charles Adeiza Umar[2]*, Yonwul Jacqueline Dakyen[3], Usman Mohammad Ibrahim[4], Uchenna Stephen Nwokenna[5], Fauwzia Sanusi[6], Odira Irene Okoye[7]

Received: 10.02.2026
Revised: 16.05.2026
Accepted: 17.05.2026
Published: 25.05.2026

[1] Center for AI Accountability in Health NG, Federal Capital Territory, Nigeria; +234-7036244967; ycherima@gmail.com; ORCID: https://orcid.org/0009-0004-3724-9886

[2] Health Strategy and Leadership (HSL) Inc., Nigeria; +234-7033262284; cumar@hslhealth.pro; ORCID: https://orcid.org/0009-0001-1469-7983

[3] Independent Public Health Researcher, Nigeria; ydakyen@yahoo.com; ORCID: https://orcid.org/0009-0006-7229-4943

[4] Nigeria Centre for Disease Control and Prevention (NCDC), Nigeria; +234-8035563217; ibrahim.usman@ncdc.gov.ng; ORCID: https://orcid.org/0009-0009-9625-7671

[5] Department of Policy and Strategic Studies, University of Abuja, Federal Capital Territory, Nigeria; +234-8178867435; unwokenna2@gmail.com; ORCID: https://orcid.org/0009-0004-8219-3260

[6] Kano State Primary Health Care Management Board, Kano State, Nigeria; +234-9031568154; fawzya2012@gmail.com; ORCID: https://orcid.org/0009-0001-2832-1864

[7] Miva Open University, Nigeria; +234-8109016877; odira899@gmail.com; ORCID: https://orcid.org/0009-0008-0868-0924

* Correspondence: cumar@hslhealth.pro

Abstract

Severe malaria treatment gaps and routine immunization (RI) zero-dose childhood vulnerability are major but often independently investigated public health challenges in sub-Saharan Africa, despite the common health system and accessibility constraints. This study examined the spatial co-occurrence of hidden severe malaria burden and RI zero-dose childhood vulnerability across Kano State, Nigeria, and developed a dual vulnerability index (DVI) to support integrated intervention prioritization. An LGA-level geospatial database integrating severe malaria surveillance records, treatment coverage indicators, RI microcensus data, malaria transmission metrics, population estimates, health facility density, and socioeconomic proxies was analyzed via descriptive statistics, Spearman correlation, hotspot analysis, K-means clustering, and composite vulnerability modeling. Spatial co-occurrence was quantified via the Hidden Burden Treatment Gap Index (HBTGI), the Artesunate-Adjusted Severe Malaria Treatment Gap Index (AASMTGI), and the RI zero-dose rates, whereas the DVI integrated the malaria treatment gap and immunization deprivation indicators under alternative weighting schemes. Significant positive spatial autocorrelation was observed for hidden severe malaria burden (Moran's $I = 0.412$, $p < 0.001$), RI zero-dose vulnerability (Moran's $I = 0.339$, $p < 0.001$), and the composite co-occurrence score (Moran's $I = 0.240$, $p = 0.003$), demonstrating geographically concentrated vulnerability clusters. Gwarzo, Bichi, Rogo, Sumaila, Bagwai, Rano, Takai, Wudil, Gaya, and Dambatta emerged as the highest-priority LGAs exhibiting simultaneous high hidden malaria burdens, severe treatment gaps, and elevated RI zero-dose rates. K-means clustering identified three distinct malaria–immunization vulnerability typologies, with the most vulnerable cluster comprising 12 LGAs exhibiting an average co-occurrence score of 79.7 and RI zero-dose rates of 66.6%. Sensitivity analyses revealed that DVI rankings were robust across equal, PCA, and entropy weighting approaches. The findings demonstrate that the hidden severe malaria burden and childhood immunization deprivation ex-

hibit substantial spatial overlap in Kano State and highlight the value of the proposed DVI as a geospatial decision-support framework for targeting integrated malaria control, immunization strengthening, and primary healthcare interventions.

Keywords: Dual vulnerability index (DVI); artesunate-adjusted severe malaria treatment gap index; K-means clustering; zero-dose; Nigeria.

1. Introduction

Malaria remains one of the most important public health challenges in sub-Saharan Africa, accounting for the majority of global malaria cases and deaths. In 2023, the World Health Organization (WHO) estimated 263 million malaria cases and 597,000 malaria-related deaths worldwide, with Africa contributing approximately 94% of cases and 95% of deaths. Nigeria continues to bear the highest malaria burden globally, accounting for more than one quarter of all malaria cases and nearly one third of malaria-related deaths worldwide [1,2]. Despite substantial investments in malaria prevention, diagnosis, treatment, and surveillance, severe malaria remains a major cause of morbidity and mortality among children under five years of age in many parts of northern Nigeria [3,4].

Prompt diagnosis and treatment of severe malaria with injectable artesunate are essential for reducing mortality and preventing complications [5]. However, routine surveillance systems frequently underestimate the true burden of severe malaria because many cases remain untreated, are unreported, or are managed outside formal healthcare facilities [6,7]. This phenomenon creates a hidden severe malaria burden that is often masked by routine reporting systems and may lead to substantial underestimation of treatment needs. Recent studies have highlighted the importance of identifying treatment gaps and surveillance blind spots to improve malaria control planning and resource allocation [8,9].

Moreover, childhood immunization remains one of the most cost-effective public health interventions for reducing child mortality and preventing vaccine-preventable diseases [10]. However, millions of children worldwide remain unvaccinated or undervaccinated, particularly in low-resource settings [11]. Children who have not received any routine immunization dose, commonly referred to as zero-dose children, represent a critical indicator of health system exclusion and inequitable access to essential health services [12,13]. In Nigeria, the concentration of zero-dose children is among the highest in the world, with northern states accounting for a substantial proportion of the national burden [14,15]. Previous studies have shown that zero-dose children are frequently concentrated in geographically isolated, socioeconomically disadvantaged, and health-service-deprived communities [16,17].

Although malaria and immunization programs are often implemented independently, both are strongly influenced by common determinants, including health facility accessibility, healthcare workforce availability, socioeconomic deprivation, population mobility, insecurity, and weaknesses in primary healthcare systems [18–20]. Consequently, areas experiencing severe malaria treatment deficiencies may also exhibit poor immunization coverage and elevated concentrations of zero-dose drugs in children. Identifying these overlapping vulnerabilities is important because children living in such settings face compounded health risks resulting from both inadequate malaria case management and insufficient preventive healthcare services.

Recent advances in geospatial health analytics have demonstrated the value of integrating multiple health indicators to identify priority intervention areas and support evidence-based decision-making [21–23]. Spatial hotspot analysis, cluster analysis, and composite vulnerability indices have increasingly been used to characterize disease burden, healthcare access inequalities, and population vulnerability across diverse public health contexts [24–26]. However, few studies have explicitly examined the geographic overlap between the hidden severe malaria burden and childhood immunization deprivation, particularly in high-burden settings such as northern Nigeria. Further-

more, no known study has developed a composite framework that simultaneously quantifies severe malaria treatment gaps and routine immunization vulnerability at the local government area level.

Kano State represents a particularly important setting for such analysis. As one of Nigeria's most populous states, Kano experiences intense malaria transmission and persistent routine immunization challenges [3]. The state also contains large populations of underfive children and significant geographic variation in health outcomes. Understanding where hidden severe malaria burdens and zero-dose childhood vulnerability cooccur can support more efficient targeting of limited public health resources and strengthen integrated child health interventions.

The present study therefore aims to (1) identify local government areas where hidden severe malaria burdens overlap with high concentrations of routine immunization zero-dose children and (2) develop a dual vulnerability index (DVI) that combines severe malaria treatment gaps and childhood immunization deprivation into a single spatial decision-support framework. By integrating malaria surveillance indicators, treatment-gap metrics, and immunization vulnerability measures within a geospatial analytical framework, this study provides new evidence on the geography of compounded child health vulnerability in Kano State. The findings demonstrate that hidden severe malaria burden and zero-dose childhood vulnerability exhibit significant spatial overlap and clustering and that the proposed dual vulnerability index offers a practical tool for identifying priority LGAs requiring coordinated malaria control and immunization strengthening interventions.

2. Materials and methods

2.1 Study area

The study was conducted in Kano State, northwestern Nigeria, one of the most populous states in the country and a major center of economic, commercial, and agricultural activity. Kano State lies approximately between latitudes 10°30′N and 13°00′N and longitudes 7°30′E and 10°00′E, covering an area of approximately 20,131 km². The state is administratively divided into 44 local government areas (LGAs), which constitute the primary spatial units used in this analysis (Figure 1).

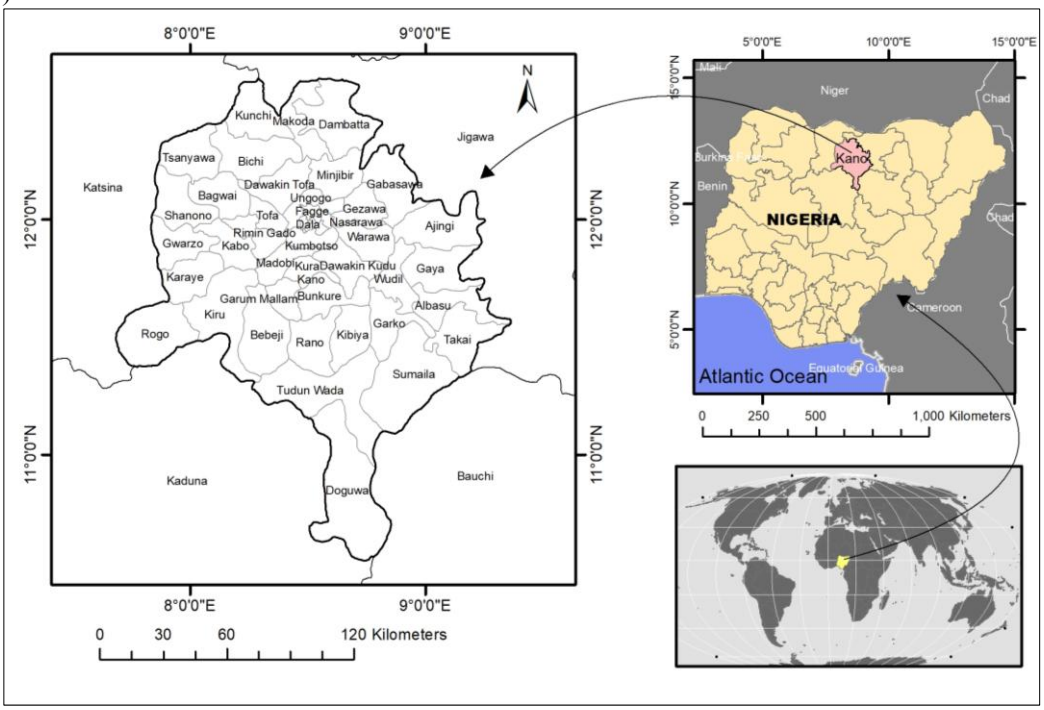

Figure 1. Location of Kano State within Nigeria and the administrative boundaries of the 44 local government areas (LGAs) used in the analysis.

Kano State experiences a tropical savanna climate characterized by distinct wet and dry seasons. The rainy season typically extends from May to October, whereas the dry season lasts from November to April (Figure 2).

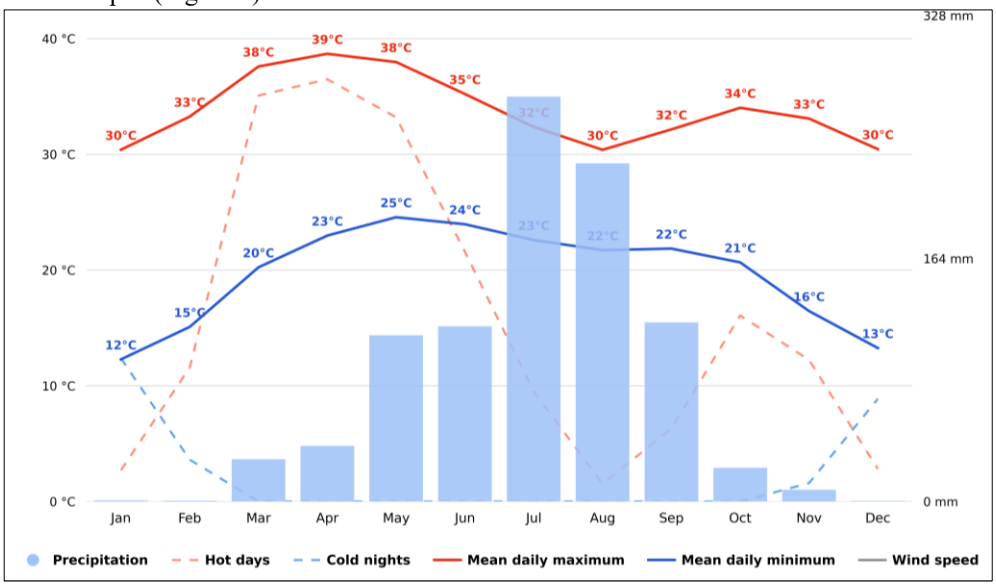

Figure 2. Mean monthly precipitation and temperature patterns in Kano State, Nigeria, for the period 2015–2025 were derived from NASA POWER data [34].

The annual rainfall generally ranges from 600 to 1,200 mm, with increasing precipitation in southern parts of the state. The mean annual temperatures are generally high throughout the year, often exceeding 25°C, creating favorable environmental conditions for malaria transmission. Seasonal variations in rainfall, temperature, and humidity influence mosquito breeding habitats and contribute to temporal fluctuations in malaria incidence.

The state has an estimated population exceeding 16 million people and contains one of the largest concentrations of children under five years of age in Nigeria. Rapid population growth, urban expansion, socioeconomic disparities, and variations in healthcare accessibility contribute to substantial heterogeneity in health outcomes across LGAs. Although Kano possesses an extensive primary healthcare network, challenges related to service accessibility, healthcare utilization, routine immunization coverage, and severe malaria case management persist in several parts of the state.

2.2 Study Design and Analytical Workflow

The framework integrates severe malaria surveillance data, routine immunization microcensus information, population and settlement characteristics, malaria transmission indicators, health facility accessibility measures, and socioeconomic proxies within a unified LGA-level geospatial database. Two complementary vulnerability pathways are examined: (i) hidden severe malaria burden represented by the hidden burden treatment gap index (HBTGI), the artesunate-adjusted severe malaria treatment gap index (AASMTGI), and severe malaria treatment gaps; and (ii) childhood immunization vulnerability represented by RI zero-dose rates, numbers of zero-dose children, non-vaccination rates, and low vaccination coverage. Objective 1: To identify geographic areas where malaria treatment deficiencies spatially overlap with childhood immunization deprivation through co-occurrence mapping, hotspot detection, and cluster analysis. Objective 2 integrates malaria and immunization vulnerability dimensions into a dual vulnerability index (DVI) via alternative weighting approaches. The resulting DVI is used to classify, rank, and prioritize local government areas (LGAs) for integrated malaria control, routine immunization strengthening, and evidence-based primary healthcare microplanning (Figure 3).

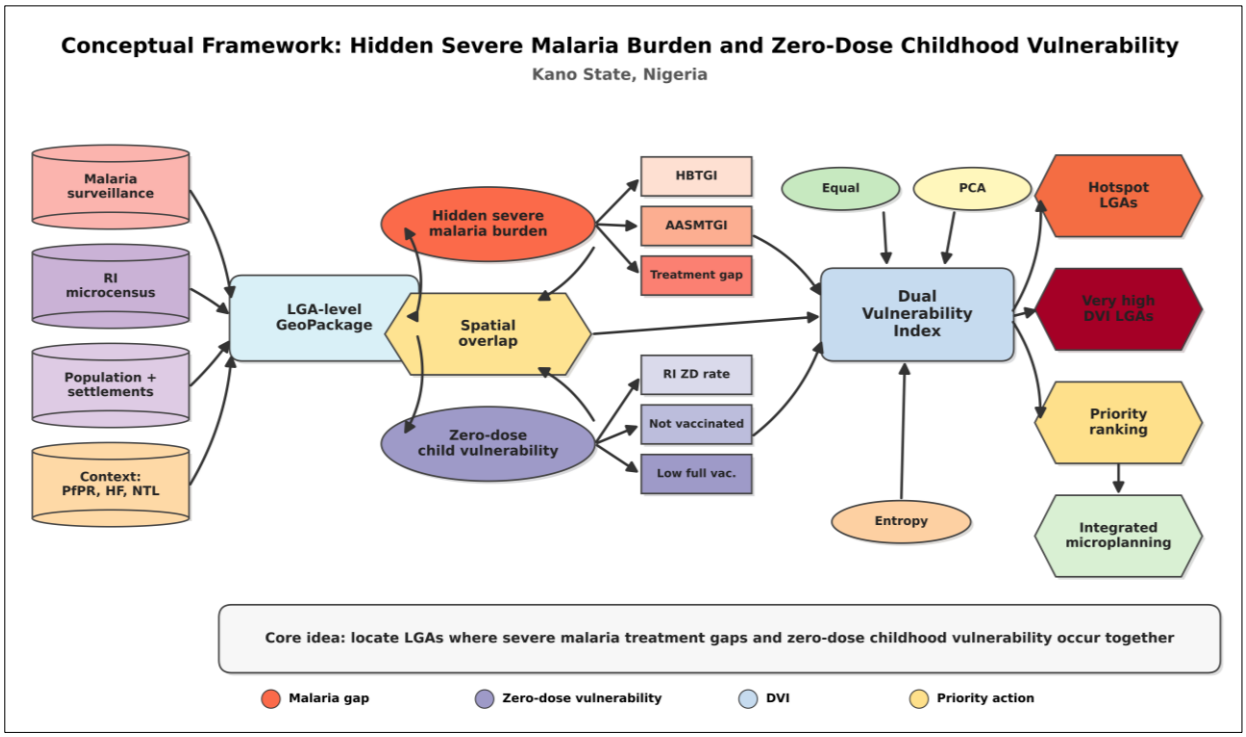

Figure 3. Conceptual framework for assessing the co-occurrence of hidden severe malaria burden and zero-dose childhood vulnerability and developing a dual vulnerability index (DVI) in Kano State, Nigeria.

2.3 Data Sources

The analysis was conducted via an integrated LGA-level geospatial database developed for Kano State, Nigeria. The database combines routine health information system records on severe malaria burden and treatment coverage, routine immunization microcensus data, malaria transmission indicators from the Malaria Atlas Project, population estimates from WorldPop, health facility data from GRID3, and socioeconomic accessibility proxies derived from VIIRS nighttime lights. All the datasets were harmonized and aggregated to the LGA level within a single GeoPackage, which served as the master analytical database for spatial co-occurrence analysis and dual vulnerability index (DVI) development.

Table 1 Data Summary

Data Name	Data Type	Purpose	Source
Severe Malaria Cases	Vector (LGA)	Severe malaria burden	RHIS/DHIS2 [27]
Severe Malaria Treated with Artesunate	Vector (LGA)	Treatment gaps	RHIS/DHIS2 [27]
Hidden Burden Treatment Gap Index	Indicator	Hidden severe malaria burden	Derived
Artesunate-Adjusted Severe Malaria Treatment Gap Index (AASMTGI)	Derived LGA Indicator	Assessment of severe malaria treatment deficiencies	Derived from RHIS/DHIS2
RI Zero-Dose Children	Vector (LGA)	Identification of missed children	RI Microcensus [28]
RI Zero-Dose Rate (U5)	Indicator	Immunization deprivation	RI Microcensus [28]
Not Vaccinated Children	Vector (LGA)	Immunization exclusion	RI Microcensus [28]
Not Vaccinated Rate (U5)	Indicator	Immunization vulnerability	RI Microcensus [28]
Fully Vaccinated Rate (U5)	Derived	Immunization performance	RI Microcensus [28]
Under-Five Population	Aggregated	Denominator for immunization	RI Microcensus [28]
Household Count	Aggregated	Population contextualization	RI Microcensus [28]

Settlement Count	Aggregated	Settlement distribution	RI Microcensus [28]
Health Facilities	Vector	Service availability	GRID3 [29]
Population 2025	Raster	Population exposure	WorldPop [30]
PfPR 2024	Raster	Malaria transmission intensity	Malaria Atlas [31]
PfIR 2024	Raster	Malaria infection intensity	Malaria Atlas [31]
PfMR 2024	Raster	Malaria mortality burden	Malaria Atlas [31]
PfIC 2024	Raster	Clinical malaria incidence	Malaria Atlas [31]
PfMC 2024	Raster	Clinical malaria burden	Malaria Atlas [31]
VIIRS Nighttime Lights 2025	Raster	Socioeco. development proxy	NASA/NOAA VIIRS [32]
Administrative Boundaries	Vector	Spatial aggregation and mapping	OCHA Nigeria [33]

Abbreviations: HBTGI = Hidden Burden Treatment Gap Index; AASMTGI = Artesunate-Adjusted Severe Malaria Treatment Gap Index; RI = Routine Immunization; U5 = Under-Five Children; PfPR = *Plasmodium falciparum* Parasite Rate; PfIR = *Plasmodium falciparum* Infection Rate; PfMR = *Plasmodium falciparum* Mortality Rate; PfIC = *Plasmodium falciparum* Incidence Cases; PfMC = *Plasmodium falciparum* Malaria Cases; RHIS = Routine Health Information System; DHIS2 = District Health Information System 2; GRID3 = Geo-Referenced Infrastructure and Demographic Data for Development; VIIRS = Visible Infrared Imaging Radiometer Suite.

2.3 Data Preprocessing

2.3.1 Spatial Cooccurrence Analysis of Hidden Severe Malaria Burden and Zero-Dose Childhood Vulnerability

To identify local government areas (LGAs) where the hidden severe malaria burden overlaps with routine immunization (RI) zero-dose childhood vulnerability, a spatial co-occurrence framework was developed using three primary indicators: the Hidden Burden Treatment Gap Index (HBTGI), the Artesunate-Adjusted Severe Malaria Treatment Gap Index (AASMTGI), and the RI zero-dose rate among underfive children (RI_ZD_Rate_U5).

Descriptive statistics, including the mean, standard deviation, median, minimum, maximum, skewness, and kurtosis, were calculated for all malaria, immunization, demographic, and contextual variables. Relationships among indicators were evaluated via Spearman's rank correlation coefficient because of the nonnormal distribution and ordinal characteristics of several vulnerability measures.

To facilitate comparisons among variables measured at different scales, all indicators were standardized via min–max normalization:

$$X_{norm} = \frac{X_i - X_{min}}{X_{max} - X_{min}} \quad (1)$$

where X_i is the observed value, X_{min} is the minimum observed value, and X_{max} is the maximum observed value.

A composite co-occurrence score (COS) was then calculated as the arithmetic mean of the normalized HBTGI, normalized AASMTGI, and normalized RI zero-dose rate:

$$COS = \frac{HBTGI_{norm} + AASMTGI_{norm} + RIZD_{norm}}{3} \times 100 \quad (2)$$

where larger values indicate greater overlap between the hidden severe malaria burden and childhood immunization deprivation.

To account for both the intensity and magnitude of immunization deprivation, a count-weighted co-occurrence score was additionally computed by incorporating the normalized number of RI zero-dose children:

$$COS_{CW} = \frac{HBTGI_{norm} + AASMTGI_{norm} + RIZD_{Rate,norm} + RIZD_{Count,norm}}{4} \times 100 \quad (3)$$

LGAs were subsequently classified into five co-occurrence categories (very low, low, moderate, high, and very high) via quintile classification.

To identify priority intervention areas, upper quartile (75th percentile) thresholds were calculated for the HBTGI, AASMTGI, treatment gap, and RI zero-dose rates. LGAs exceeding the 75th percentile for HBTGI, AASMTGI, and the RI zero-dose rate were classified as triple overlap areas, whereas LGAs simultaneously exceeding the 75th percentile for HBTGI, AASMTGI, the treatment gap, and the RI zero-dose rate were classified as quadruple overlap areas. These areas represent locations experiencing concurrent hidden malaria burdens, severe malaria treatment deficiencies, and childhood immunization deprivation.

Spatial autocorrelation of vulnerability patterns was assessed via Global Moran's I:

$$I = \frac{n}{W} \frac{\sum_i \sum_j w_{ij} (x_i - \dot{x})(x_j - \dot{x})}{\sum_i (x_i - \dot{x})^2} \quad (4)$$

where n is the number of LGAs, w_{ij} represents the spatial weight between neighboring LGAs, and W is the sum of all spatial weights.

Local clustering was evaluated via the Getis–Ord G_i^* statistic to identify statistically significant hotspots and coldspots of cooccurring vulnerability:

$$G_i^* = \frac{\sum_j w_{ij} x_j - \dot{X} \sum_j w_{ij}}{S \sqrt{\frac{n \sum_j w_{ij}^2 - (\sum_j w_{ij})^2}{n-1}}} \quad (5)$$

LGAs were classified as hotspot or coldspot areas at 90%, 95%, and 99% confidence levels.

To further identify distinct malaria–immunization vulnerability typologies, K-means cluster analysis was applied via four standardized indicators: HBTGI, AASMTGI, treatment gap, and the RI zero-dose rate. Three clusters were specified to differentiate LGAs exhibiting low, moderate, and high combined vulnerability profiles.

Finally, all LGAs were ranked according to their co-occurrence score to identify locations requiring integrated malaria case-management strengthening and routine immunization recovery interventions.

2.3.2 Development of the dual vulnerability index (DVI)

A dual vulnerability index (DVI) was developed to quantify the combined burden of severe malaria treatment deficiencies and childhood immunization deprivation across Kano State LGAs.

The malaria vulnerability dimension consisted of the following:

- Hidden Burden Treatment Gap Index (HBTGI)
- Artesunate-Adjusted Severe Malaria Treatment Gap Index (AASMTGI)
- Severe malaria treatment gap

The immunization vulnerability dimension consisted of the following:

- RI zero-dose rate among children under five
- Rate of vaccination among children under five years of age
- Fully vaccinated rate among children under five years of age

Because higher full vaccination coverage indicates lower vulnerability, this variable was reverse normalized:

$$FV_{inv} = 1 - FV_{norm} \quad (6)$$

where FV_{norm} represents the normalized fully vaccinated rate.

All indicators were transformed to a common 0–1 scale via min–max normalization.

The malaria vulnerability dimension (MVD) was calculated as follows:

$$MVD = \frac{HBTGI_{norm} + AASMTGI_{norm} + TG_{norm}}{3}$$

where TG denotes the treatment gap indicator.

The immunization vulnerability dimension (IVD) was calculated as follows:

$$IVD = \frac{RIZD_{norm} + NV_{norm} + FV_{inv}}{3} \quad (7)$$

where $RIZD$ is the RI zero-dose rate, NV is the unvaccinated rate, and FV_{inv} is the inverse normalized fully vaccinated rate.

The primary dual vulnerability index was computed via an equal-weighting approach:

$$DVI_{EW} = \frac{MVD + IVD}{2} \times 100 \quad (8)$$

Higher DVI values indicate greater combined vulnerability to hidden severe malaria burden and immunization deprivation.

To assess methodological robustness, two alternative weighting approaches were implemented.

For principal component analysis (PCA) weighting, variable weights were derived from the absolute loadings of the first principal component:

$$w_i = \frac{|\, L_i \,|}{\sum |\, L_i \,|} \quad (9)$$

where L_i is the loading of variable i.

The PCA-weighted index was calculated as follows:

$$DVI_{PCA} = \sum_{i=1}^{n} w_i X_i \quad (10)$$

where X_i represents the normalized indicator values.

For entropy weighting, indicator proportions were calculated as follows:

$$p_{ij} = \frac{x_{ij}}{\sum_i x_{ij}} \quad (11)$$

The entropy values were then estimated as follows:

$$E_j = -\frac{1}{\ln(n)} \sum_i p_{ij} \ln(p_{ij}) \quad (12)$$

The degree of diversification was computed as follows:

$$d_j = 1 - E_j \quad (13)$$

and indicator weights were obtained from:

$$w_j = \frac{d_j}{\sum d_j} \quad (14)$$

The entropy-weighted DVI was then calculated as:

$$DVI_{Entropy} = \sum_{j=1}^{n} w_j X_j \quad (15)$$

The equal-weighted DVI was adopted as the primary index because of its transparency, interpretability, and suitability for public health decision-making. PCA-weighted and entropy-weighted indices were used exclusively for sensitivity analysis.

The final DVI scores were classified into five categories (very low, low, moderate, high, and very high) via quintile classification. LGAs were subsequently ranked according to DVI values to identify priority locations requiring integrated malaria treatment-gap reduction and routine immunization strengthening interventions. Sensitivity analysis was performed by comparing LGA rankings derived from equal-weighting, PCA-weighting, and entropy-weighting approaches via Spearman rank correlation coefficients.

3. Results

3.1 Spatial Co-Occurrence of Hidden Severe Malaria Burden and Zero-Dose Childhood Vulnerability

3.1.1 Descriptive characteristics of malaria and immune vulnerability indicators

Descriptive statistics revealed substantial spatial heterogeneity in severe malaria burden, treatment gaps, and childhood immunization deprivation across Kano State LGAs. The mean number of severe malaria cases was 4338 cases per LGA, whereas the mean treatment gap was 555 cases, indicating considerable variation in access to effective severe malaria treatment. The Hidden Burden Treatment Gap Index (HBTGI) averaged 60.2 (range: 0–100), suggesting substantial differences in the hidden severe malaria burden among LGAs. Similarly, the RI zero-dose indicators exhibited marked variability, reflecting uneven access to routine immunization services across the state (Figure 4).

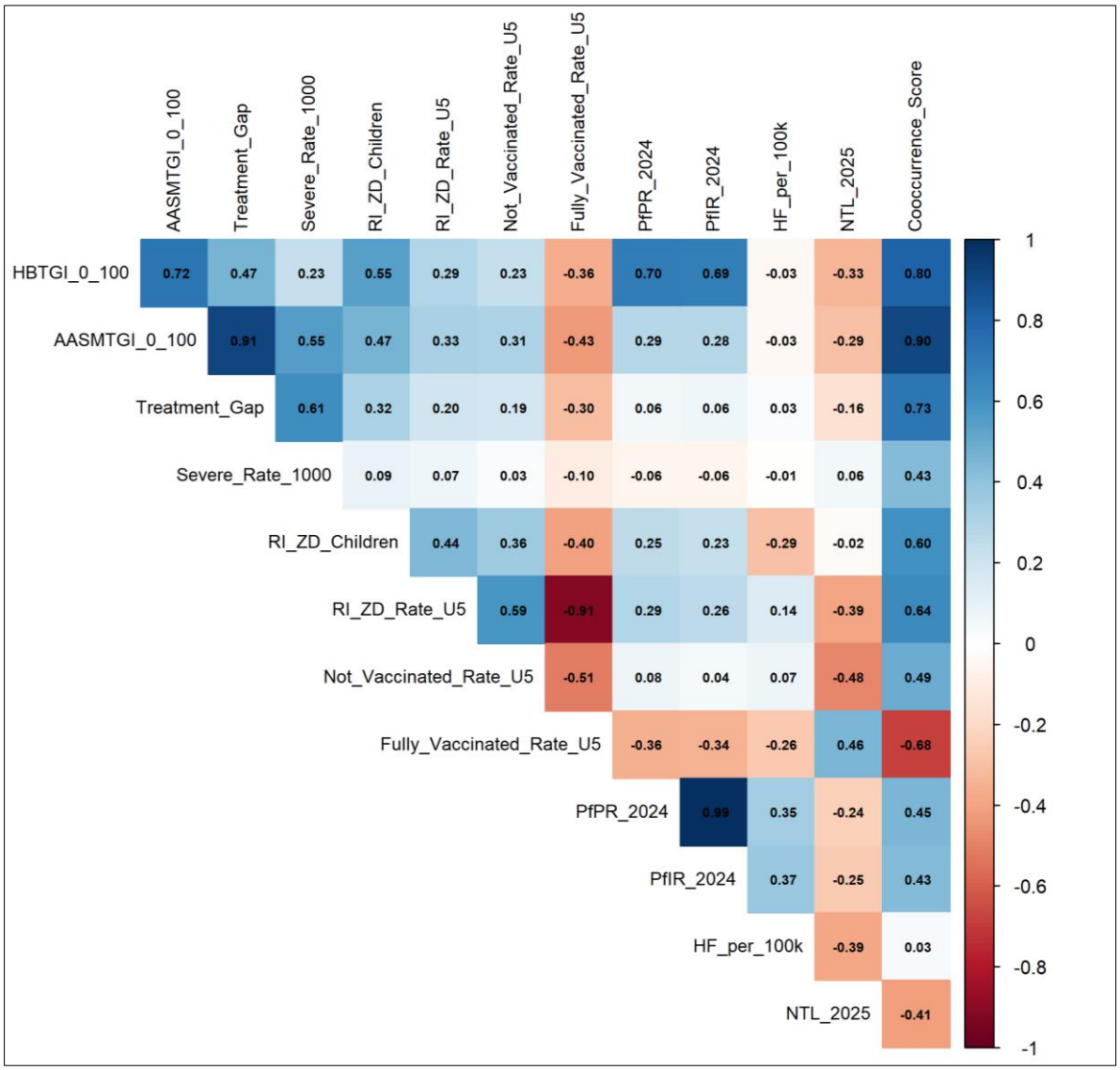

Figure 4. Correlation matrix showing relationships among hidden severe malaria burden indicators, treatment-gap metrics, immunization deprivation variables, malaria transmission indicators, health facility density, and socioeconomic accessibility proxies across Kano State LGAs.

3.1.2 Relationships between Hidden Severe Malaria Burden and Zero-Dose Childhood Vulnerability

Spearman correlation analysis revealed significant associations between malaria treatment gap indicators and childhood immunization deprivation metrics. LGAs with higher hidden severe malaria burdens and larger treatment gaps generally tended to have higher concentrations of RI zero-dose children and elevated nonvaccination rates. These findings suggest that severe malaria treatment deficiencies and routine immunization deprivation are influenced by similar health systems, accessibility, and service-delivery constraints.

The scatterplot analysis further revealed a positive relationship between the hidden burden treatment gap index (HBTGI) and the RI zero-dose rates, indicating that LGAs with greater hidden severe malaria burdens frequently experience poorer routine immunization coverage (Figure 5).

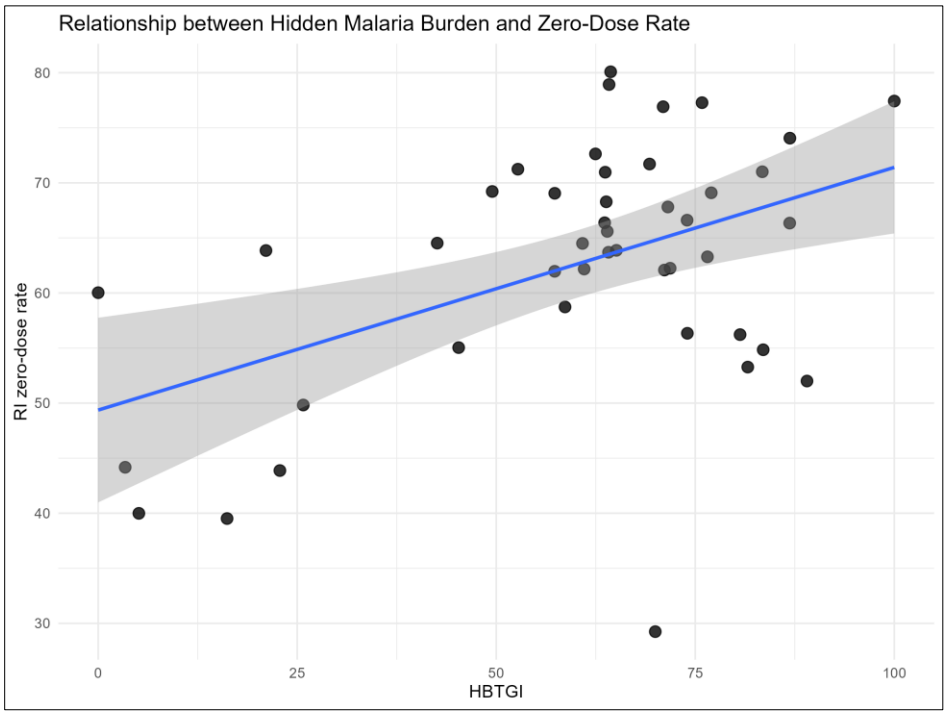

Figure 5. Scatterplot illustrating the relationship between the Hidden Burden Treatment Gap Index (HBTGI) and the RI zero-dose rate among underfive children across Kano State LGAs.

3.1.3 Spatial Distribution of Hidden Severe Malaria Burden and Zero-Dose Vulnerability

Marked spatial variation was observed in the distributions of hidden severe malaria burdens, artesunate-adjusted treatment gaps, and RI zero-dose vulnerability across Kano State. Several LGAs presented consistently elevated HBTGI and AASMTGI values, indicating areas where severe malaria treatment needs to be adequately addressed despite ongoing malaria control efforts.

Similarly, RI zero-dose vulnerability was concentrated in specific LGAs, suggesting persistent inequities in routine immunization service delivery. The spatial overlap of these indicators highlights geographic areas where children are simultaneously exposed to elevated severe malaria risk and inadequate immunization coverage (Figure 6).

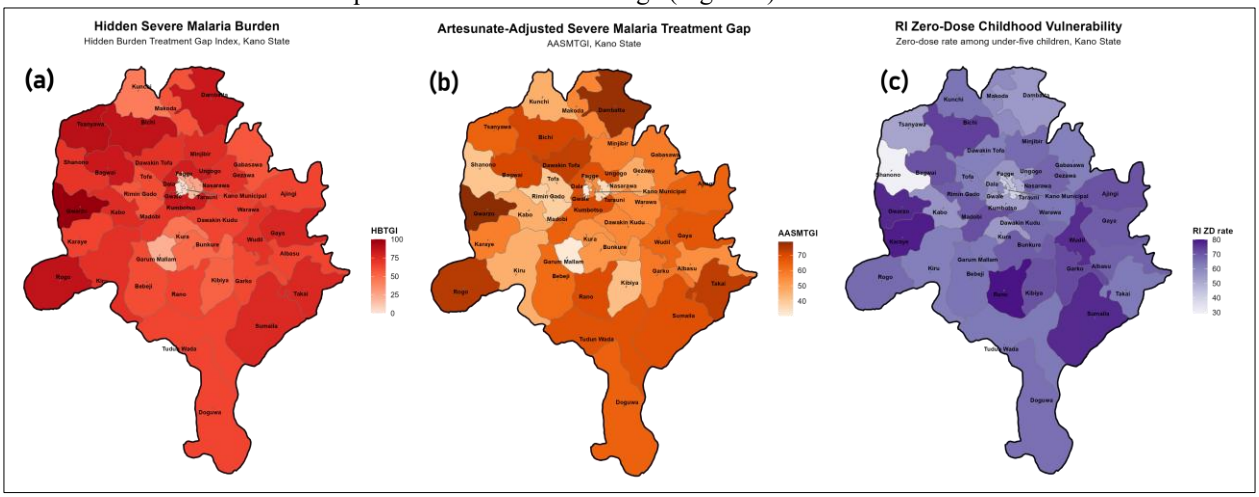

Figure 6. (a) Spatial distribution of the Hidden Burden Treatment Gap Index (HBTGI), (b) Artesunate-Adjusted Severe Malaria Treatment Gap Index (AASMTGI) and (c) RI zero-dose rates among underfive children across Kano State LGAs.

3.1.4 Cooccurrence Patterns and Priority Intervention LGAs

The composite co-occurrence score revealed substantial overlap between the hidden severe malaria burden and childhood immunization deprivation across Kano State. LGAs classified within the highest co-occurrence category represent areas where severe malaria treatment deficiencies and immunization service gaps converge.

The highest-ranking LGAs on the basis of the co-occurrence score were Gwarzo, Bichi, Rogo, Sumaila, Bagwai, Rano, Takai, Wudil, Gaya, and Dambatta. These LGAs presented the greatest combined burden of hidden severe malaria, artesunate-adjusted treatment gaps, and RI zero-dose vulnerability and therefore represent priority targets for integrated intervention strategies (Figure 7).

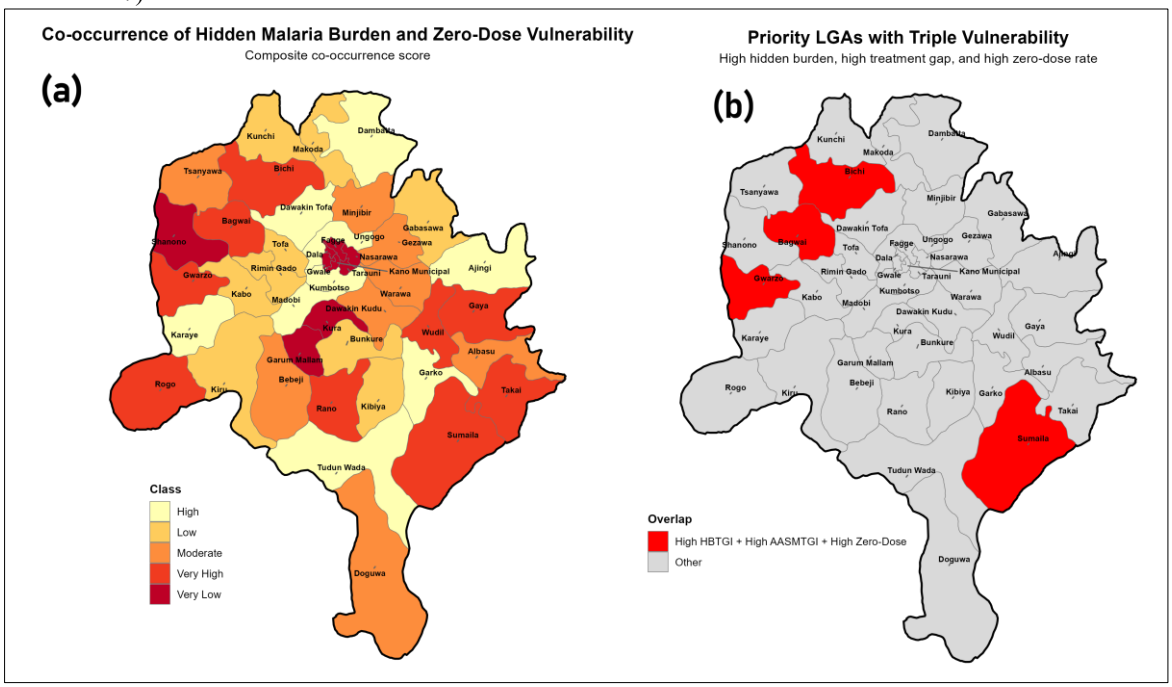

Figure 7. (a) Cooccurrence map showing the combined spatial distribution of hidden severe malaria burden and RI zero-dose childhood vulnerability. (b) Triple overlap label across Kano State LGAs.

3.1.5 Malaria–Immunization Vulnerability Typologies

K-means cluster analysis identified three distinct malaria–immunization vulnerability typologies across Kano State. Cluster 1 consisted of eight LGAs characterized by relatively low co-occurrence scores and lower RI zero-dose rates. Cluster 2 contained twenty-four LGAs exhibiting moderate vulnerability levels, whereas Cluster 3 comprised twelve LGAs with the highest average co-occurrence score (79.7) and elevated RI zero-dose rates (66.6%), representing the most vulnerable group of LGAs. These clusters provide an operational framework for tailoring intervention strategies according to local vulnerability profiles (Figure 8).

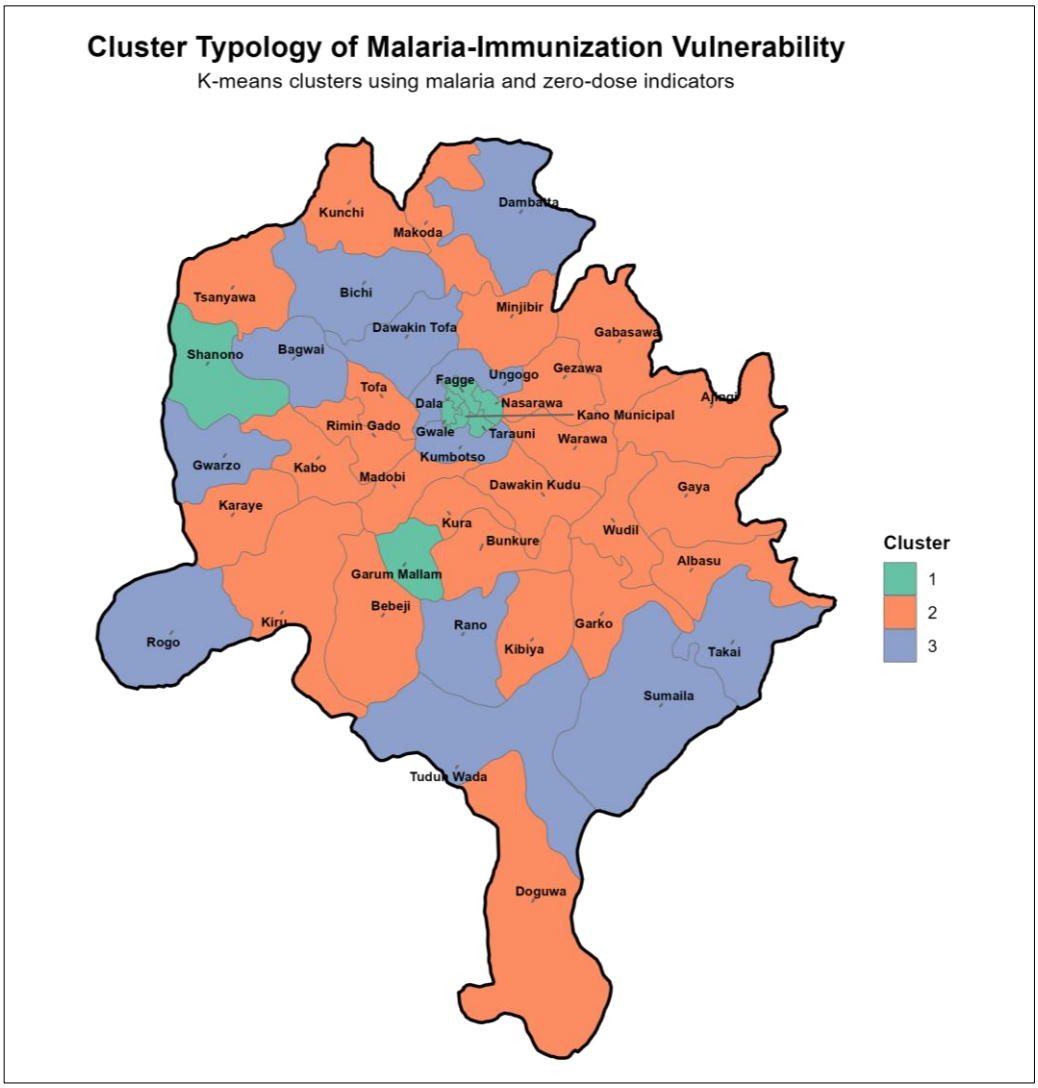

Figure 8. K-means cluster typology of malaria immunization vulnerability across Kano State LGAs on the basis of the HBTGI, AASMTGI, treatment gap, and RI zero-dose rate.

3.2 Development and spatial distribution of the dual vulnerability index (DVI)

3.2.1 Malaria and Immunization Vulnerability Dimensions

The dual vulnerability index (DVI) was developed by integrating two complementary dimensions of child health vulnerability: malaria treatment gap vulnerability and childhood immunization deprivation. The malaria dimension incorporated the Hidden Burden Treatment Gap Index (HBTGI), the Artesunate-Adjusted Severe Malaria Treatment Gap Index (AASMTGI), and treatment-gap indicators, whereas the immunization dimension incorporated RI zero-dose rates, nonvaccinated rates, and inverse full-vaccination coverage (Figure 9).

The spatial distribution of the malaria vulnerability dimension revealed substantial heterogeneity across Kano State, with several LGAs exhibiting elevated hidden severe malaria burdens and treatment deficiencies. Similarly, the immunization vulnerability dimension highlighted LGAs characterized by high concentrations of zero-dose and nonvaccinated children. The spatial congruence between these dimensions indicates that malaria treatment deficiencies and immunization deprivation frequently occur within the same geographic settings.

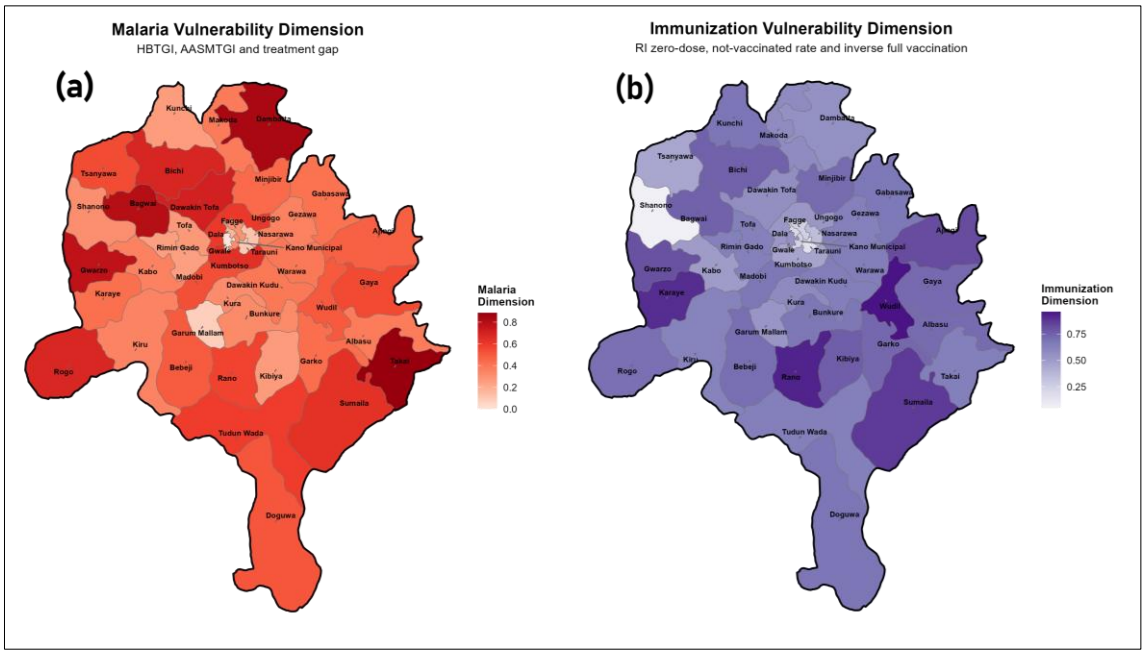

Figure 9. (a) Spatial distribution of the malaria vulnerability dimension derived from the HBTGI, AASMTGI, and treatment-gap indicators. (b) Spatial distribution of the immunization vulnerability dimension derived from the RI zero-dose rates, nonvaccination rates, and inverse full-vaccination coverage across the Kano State LGAs.

3.2.2 Principal Component and Entropy Weighting Assessment

Principal component analysis (PCA) was performed to evaluate the relative contributions of individual indicators to the overall vulnerability structure. The scree plot indicated that the first principal component explained the largest proportion of variance among the six vulnerability indicators, supporting its use for deriving PCA-based weights (Figure 10).

Entropy weighting was additionally applied to quantify the information contribution of each indicator. Variables exhibiting greater spatial differentiation across LGAs received larger entropy weights, reflecting their stronger discriminatory power in identifying vulnerability patterns.

The comparison of PCA-derived and entropy-derived weights demonstrated that the relative influence of individual indicators varied moderately across weighting approaches. Nevertheless, all methods consistently emphasized the importance of the treatment gap and immunization-deprivation indicators in determining overall vulnerability.

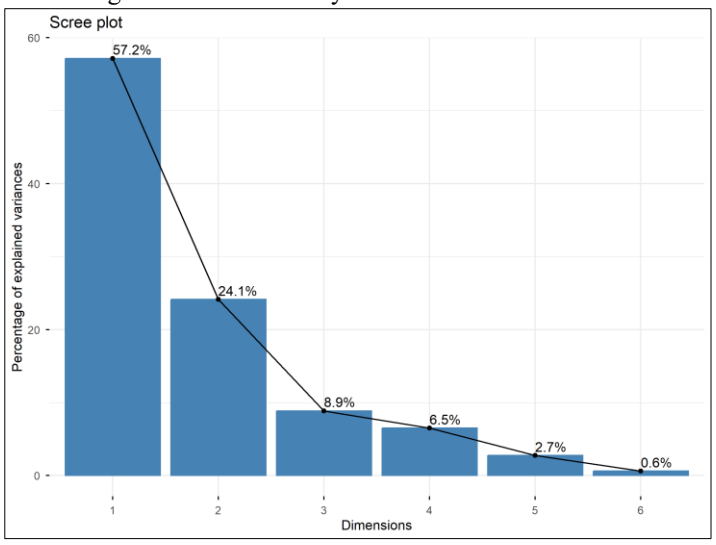

Figure 10. PCA scree plot showing the proportion of variance explained by successive principal components used in the construction of the PCA-weighted dual vulnerability index.

3.2.3 Spatial distribution of the dual vulnerability index

The equal-weighted dual vulnerability index (DVI) integrates the malaria and immunization vulnerability dimensions into a single composite measure ranging from 0--100. Higher DVI values indicate that LGAs experience simultaneous hidden severe malaria burdens, severe malaria treatment deficiencies, and childhood immunization deprivation.

The continuous DVI surface revealed pronounced spatial heterogeneity across Kano State. Several LGAs presented substantially elevated DVI values, indicating compounded public health vulnerability requiring integrated intervention strategies. The classification of DVI values into five categories (very low, low, moderate, high, and very high) further highlighted geographic disparities in vulnerability levels (Figure 11).

LGAs classified within the very high category represent locations where children face the greatest combined risks arising from inadequate severe malaria treatment and insufficient immunization coverage.

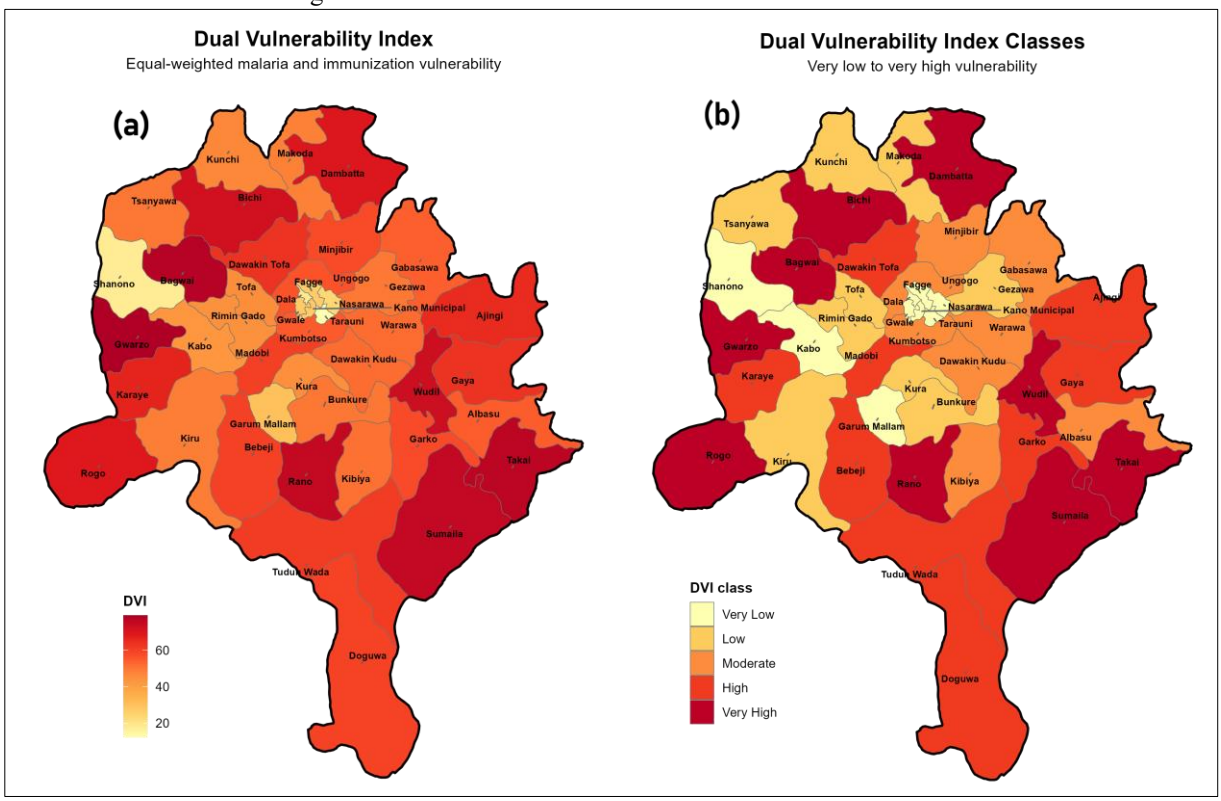

Figure 11. (a) Continuous spatial distribution of the dual vulnerability index (DVI). (b) Classification of Kano state LGAs into very low, low, moderate, high, and very high DVI categories.

3.2.4 Priority LGAs for Integrated Malaria and Immunization Interventions

Ranking of LGAs according to DVI values revealed the areas experiencing the greatest combined malaria and immunization vulnerability. The highest-ranked LGAs presented elevated hidden severe malaria burdens, substantial treatment gaps, high RI zero-dose rates, and low vaccination coverage. These LGAs represent priority locations for integrated intervention programmes involving severe malaria case-management strengthening, injectable artesunate availability, immunization recovery campaigns, and intensified community outreach.

The top-ranked LGAs should therefore be considered strategic targets for coordinated malaria and immunization investments aimed at reducing both disease burden and service-delivery inequities (Figure 12).

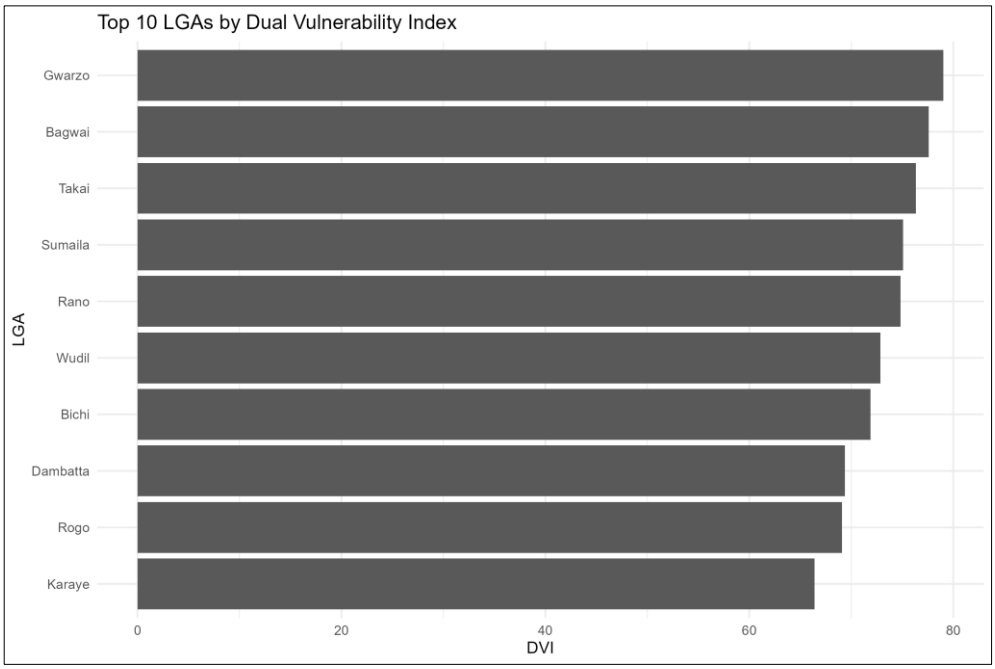

Figure 12. Top ten LGAs ranked according to the Dual Vulnerability Index, highlighting priority intervention areas requiring integrated malaria and immunization responses.

3.2.5 Sensitivity analysis of alternative weighting approaches

A sensitivity analysis was conducted to evaluate the robustness of DVI rankings under alternative weighting schemes. Comparisons between equal weighting and PCA weighting demonstrated a strong positive relationship, indicating substantial consistency in LGA rankings regardless of the weighting method used. Similarly, comparisons between equal weighting and entropy weighting showed strong agreement, suggesting that the identification of priority LGAs was largely insensitive to the weighting approach employed.

The strong concordance among weighting methods indicates that the spatial patterns of combined malaria and immunization vulnerability are stable and robust. Consequently, the equal-weighted DVI was retained as the primary operational index because of its transparency, ease of interpretation, and suitability for public health decision-making (Figure 13).

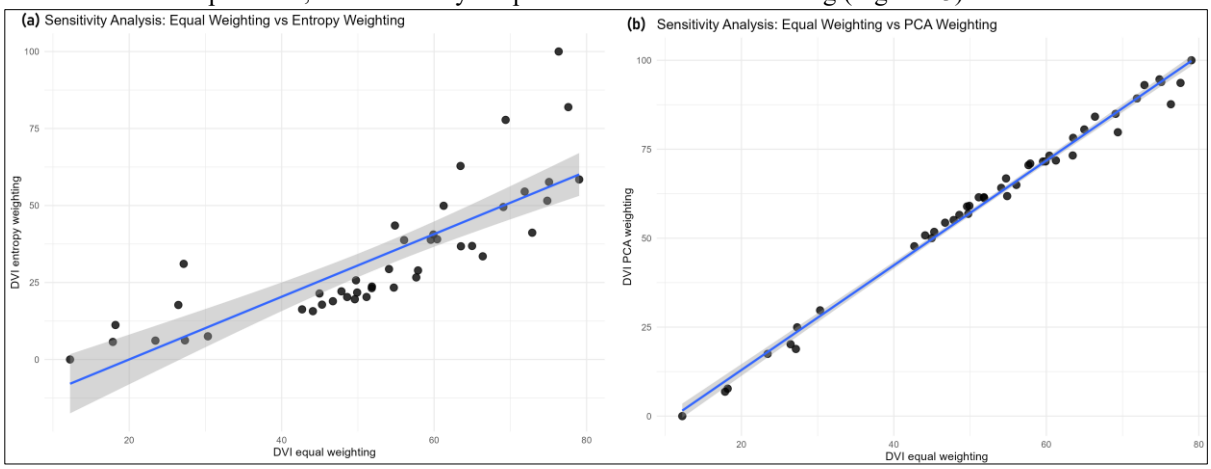

Figure 13. (a) Relationship between equal-weighted and PCA-weighted dual vulnerability index scores. (b) Relationship between equal-weighted and entropy-weighted dual vulnerability index scores across Kano State LGAs.

Overall, the sensitivity analysis demonstrated that priority intervention LGAs remain largely consistent across alternative weighting approaches, thereby increasing confidence in the robustness of the proposed dual vulnerability index framework for integrated malaria and immunization planning.

4. Discussion

This study provides evidence that the hidden severe malaria burden and childhood immunization deprivation are not randomly distributed across Kano State but instead exhibit clear spatial concentration and overlap. The significant clustering detected through Moran's I and hotspot analyses suggests that malaria treatment deficiencies and routine immunization gaps are shaped by common geographic and health-system factors operating at the local level. These findings support the hypothesis that populations experiencing barriers to timely severe malaria treatment are often the same populations facing limited access to routine immunization services.

The observed co-occurrence patterns have important implications for public health planning. Traditionally, malaria control and immunization programs are implemented through separate operational frameworks, funding streams, and monitoring systems. However, the identification of LGAs characterized by simultaneously high HBTGI, elevated treatment gaps, and high RI zero-dose rates indicates that these programs frequently target overlapping vulnerable populations. Similar patterns of geographic overlap between multiple child health risks have been reported in studies examining healthcare accessibility, vaccination inequalities, and infectious disease burdens across sub-Saharan Africa [35–37]. The present findings extend this evidence by demonstrating that severe malaria treatment gaps can serve as an additional indicator of broader health-service deprivation.

Hotspot analysis revealed that vulnerability was concentrated in specific geographic clusters rather than dispersed uniformly across the state. Such clustering is likely associated with variations in health facility accessibility, service readiness, healthcare workforce distribution, transportation infrastructure, and socioeconomic conditions. Previous studies have shown that geographic accessibility remains one of the strongest determinants of both treatment-seeking behavior and childhood vaccination uptake in low-resource settings [38,39]. Communities located farther from functional health facilities often experience delayed care seeking for severe malaria and reduced participation in routine immunization programmes. Consequently, the spatial hotspots identified in this study may represent areas where structural barriers simultaneously affect multiple child-health services.

The cluster analysis further demonstrated the existence of distinct malaria–immunization vulnerability typologies across Kano State. Rather than representing a simple gradient of risk, LGAs appeared to form groups characterized by different combinations of treatment gaps and immunization deprivation. This finding highlights the importance of adopting differentiated intervention strategies. High-vulnerability clusters may require intensive integrated outreach services, whereas moderate-vulnerability clusters may benefit from targeted service strengthening and community engagement interventions. Such stratified approaches have been recommended for improving the efficiency of public health investments in resource-constrained environments [40].

A major contribution of this study is the development of the dual vulnerability index (DVI), which integrates severe malaria treatment gaps and childhood immunization deprivation into a single operational metric. Composite vulnerability indices have been increasingly used to support public health decision-making because they simplify complex multidimensional information into interpretable measures that can guide resource allocation [41,42]. The DVI developed here demonstrated strong consistency across equal-weighting, PCA-weighting, and entropy-weighting approaches, suggesting that the resulting vulnerability patterns are robust and not driven by methodological assumptions regarding indicator weighting. This stability increases confidence in the utility of the index as a practical planning tool for programme managers and policymakers.

The integration of malaria and immunization indicators within a common analytical framework also aligns with the growing global emphasis on primary healthcare strengthening and integrated service delivery. Increasing evidence suggests that vertical disease programs may achieve greater effectiveness when interventions are coordinated through shared geographic targeting mechanisms [43,44]. In the context of Kano State, the DVI provides an opportunity to identify locations where integrated malaria case management, injectable artesunate availability, routine im-

munization recovery activities, and community-based outreach could generate synergistic health benefits.

The findings also demonstrate the value of combining routine surveillance data with microcensus-derived immunization indicators. Routine health information systems often provide extensive temporal coverage but may underrepresent populations with limited healthcare utilization. Conversely, microcensus approaches can capture vulnerable populations that remain largely invisible within facility-based reporting systems. By integrating these complementary data sources, the present study offers a more comprehensive representation of child-health vulnerability than would be possible when using either source independently [45].

Several limitations should be acknowledged. First, the analysis was conducted at the LGA level and therefore may mask important intra-LGA variations in vulnerability. Localized hotspots occurring at the ward or settlement level could not be fully captured within the current framework. Second, the hidden severe malaria burden indicators were derived from routinely reported surveillance data and are therefore influenced by reporting completeness and service utilization patterns. Third, the study represents a cross-sectional assessment and does not capture seasonal or interannual changes in vulnerability patterns. Future research should investigate the temporal dynamics of malaria treatment gaps and immunization deprivation and explore how climatic, environmental, and socioeconomic factors influence the emergence of vulnerability hotspots.

Despite these limitations, this study demonstrated that the hidden severe malaria burden and childhood immunization deprivation are closely interconnected geographic phenomena. The identification of overlapping hotspots and the development of a robust dual vulnerability index provide actionable evidence for strengthening integrated child–health programs. Future studies should evaluate the application of the DVI at finer spatial scales and assess its effectiveness as a tool for malaria control, immunization recovery, and broader primary healthcare interventions. Collectively, these findings highlight the importance of moving beyond disease-specific analyses toward integrated geospatial approaches capable of identifying communities facing multiple and interacting health vulnerabilities.

Data availability statement: The data used in this study are open to access as follows:

1. WorldPop Population Data Portal
2. Malaria Atlas Project Data Explorer
3. NASA/NOAA VIIRS Nighttime Lights Data
4. OCHA Nigeria Administrative Boundaries (COD-AB NGA)

Author Contributions: Author Contributions: Conceptualization, C.A.U., Y.J.C., and Z.I.; methodology, Z.I., C.A.U., and Y.J.C.; software, Z.I.; validation, C.A.U., Y.J.C., Y.J.D., and U.M.I.; formal analysis, Z.I.; investigation, Y.J.C., C.A.U., Y.J.D., U.M.I., U.S.N., F.S., and O.I.O.; data curation, U.M.I., F.S., and Y.J.C.; visualization, Z.I.; writing—original draft preparation, Z.I. and C.A.U.; writing—review and editing, Y.J.C., Y.J.D., U.M.I., U.S.N., F.S., and O.I.O.; supervision, C.A.U.; project administration, C.A.U.; resources, Y.J.C., Y.J.D., U.M.I., U.S.N., F.S., and O.I.O. All authors have read and agreed to the published version of the manuscript.

Funding

This research received no external funding.

Informed Consent Statement

Not applicable.

Conflicts of interest

The authors declare that they have no conflicts of interest.

Abbreviations

The following abbreviations are used in this manuscript:

Abbreviation	
DVI	Dual Vulnerability Index
HBTGI	Hidden Burden Treatment Gap Index
AASMTGI	Artesunate-Adjusted Severe Malaria Treatment Gap Index
RI	Routine Immunization
LGA	Local Government Area
U5	Under-Five Children
PfPR	Plasmodium falciparum Parasite Rate
PfIR	Plasmodium falciparum Infection Rate
RHIS	Routine Health Information System
DHIS2	District Health Information System 2

References

1. World Health Organization. (2024). *World malaria report 2024*. Geneva, Switzerland: WHO.
2. World Health Organization. (2024). *Malaria 2024 country profile: Nigeria*. Geneva, Switzerland: WHO.
3. National Population Commission (NPC), & ICF. (2024). *Nigeria demographic and health survey 2023*. Abuja, Nigeria, and Rockville, MD, USA: NPC and ICF.
4. Nigeria National Malaria Elimination Programme (NMEP). (2024). *National malaria strategic plan and programme performance report*. Abuja, Nigeria.
5. World Health Organization. (2023). *WHO guidelines for malaria*. Geneva, Switzerland: WHO.
6. Weiss, D. J., Lucas, T. C. D., Nguyen, M., et al. (2019). Mapping the global prevalence, incidence, and mortality of *Plasmodium falciparum*, 2000–2017. *Nature, 576*(7786), 341–345. DOI: 10.1016/S0140-6736(25)00038-8
7. Snow, R. W., Sartorius, B., Kyalo, D., et al. (2022). The changing limits and incidence of malaria in Africa. *Nature, 610*(7933), 96–104. DOI: 10.1016/B978-0-12-394303-3.00010-4
8. Noor, A. M., Alegana, V. A., Patil, A. P., et al. (2023). Geospatial intelligence for malaria control and elimination in Africa. *The Lancet Global Health, 11*(5), e683–e692.
9. Tatem, A. J., Weiss, D. J., Gibson, H. S., et al. (2021). Integrating geospatial data for health service accessibility and disease burden assessment. *International Journal of Health Geographics, 20*(1), 1–15.
10. World Health Organization. (2020). *Immunization Agenda 2030: A global strategy to leave no one behind*. Geneva, Switzerland: WHO.
11. UNICEF. (2025). *Global childhood vaccination holds steady, yet over 14 million infants remain unvaccinated*. New York, NY: UNICEF.
12. World Health Organization. (2025). *IA2030 indicator metadata: Number of zero-dose children*. Geneva, Switzerland: WHO.
13. Beaulieu A, Ducharme J, Thibeault C, et al. The Immunization Agenda 2030 Strategy to reach zero-dose children in low-income and middle-income countries: a scoping review. *BMJ Global Health*. 2025;10(8):e018293-e018293. doi:10.1136/bmjgh-2024-018293
14. National Primary Health Care Development Agency. (2024). *National routine immunization performance report*. Abuja, Nigeria.
15. UNICEF. (2022). *UNICEF immunization roadmap 2022–2030*. New York, NY: UNICEF.
16. Utazi CE, Aheto JMK, Wigley A, et al. Mapping the distribution of zero-dose children to assess the performance of vaccine delivery strategies and their relationships with measles incidence in Nigeria. *Vaccine*. 2023;41(1):170-181. doi:10.1016/j.vaccine.2022.11.026

17. Sbarra AN, Rolfe S, Nguyen JQ, et al. Mapping routine measles vaccination in low- and middle-income countries. *Nature*. 2020;589(7842):415-419. doi:10.1038/s41586-020-03043-4
18. Fullman, N., Yearwood, J., Abay, S. M., et al. (2018). Measuring performance on the Healthcare Access and Quality Index for 195 countries and territories. *The Lancet, 391*(10136), 2236–2271.
19. Osgood-Zimmerman, A., Millear, A. I., Stubbs, R. W., et al. (2018). Mapping child growth failure in Africa between 2000 and 2015. *Nature, 555*(7694), 41–47.
20. Kano State Ministry of Health. (2024). *Kano State health sector strategic development plan*. Kano, Nigeria.
21. Cromley, E. K., & McLafferty, S. L. (2012). *GIS and public health* (2nd ed.). New York, NY: Guilford Press.
22. Noor, A. M., Alegana, V. A., Patil, A. P., et al. (2023). Geospatial intelligence for malaria control and elimination in Africa. *The Lancet Global Health, 11*(5), e683–e692.
23. Tatem, A. J., Weiss, D. J., Gibson, H. S., et al. (2021). Integrating geospatial data for health service accessibility and disease burden assessment. *International Journal of Health Geographics, 20*(1), 1–15.
24. Getis, A., & Ord, J. K. (1992). The analysis of spatial association by use of distance statistics. *Geographical Analysis, 24*(3), 189–206.
25. Anselin, L. (1995). Local indicators of spatial association—LISA. *Geographical Analysis, 27*(2), 93–115.
26. Cromley, E. K., & McLafferty, S. L. (2012). *GIS and public health* (2nd ed.). New York, NY: Guilford Press.
27. HISP Centre, University of Oslo. (2024). *District Health Information System 2 (DHIS2): Open-source health management information platform*. University of Oslo, Norway. https://dhis2.org
28. National Primary Health Care Development Agency (NPHCDA). (2024). *Routine immunization micro-census operational guidelines and implementation framework*. Abuja, Nigeria.
29. Center for International Earth Science Information Network (CIESIN), Columbia University, Novel-T, and Flowminder Foundation. (2024). *GRID3 Nigeria health facility database*. GRID3 Initiative. https://grid3.org
30. WorldPop. (2025). *Global high-resolution population denominators project*. School of Geography and Environmental Science, University of Southampton, United Kingdom. https://www.worldpop.org
31. Malaria Atlas Project. (2024). *Spatial malaria datasets for Nigeria: PfPR, PfIR, PfMR, PfIC and PfMC*. University of Oxford. https://malariaatlas.org
32. National Aeronautics and Space Administration (NASA), & National Oceanic and Atmospheric Administration (NOAA). (2025). *Visible Infrared Imaging Radiometer Suite (VIIRS) Day/Night Band nighttime lights products*. https://earthdata.nasa.gov
33. United Nations Office for the Coordination of Humanitarian Affairs (OCHA). (2024). *Nigeria administrative boundaries (Admin 0–2)*. Humanitarian Data Exchange (HDX). https://data.humdata.org
34. National Aeronautics and Space Administration (NASA). (2025). *NASA Prediction of Worldwide Energy Resources (POWER) project*. NASA Langley Research Center. https://power.larc.nasa.gov
35. Utazi, C. E., Thorley, J., Alegana, V. A., et al. (2020). Mapping vaccination coverage to explore the geography of zero-dose children in Africa. *Nature Communications, 11*, 5621.
36. Golding, N., Burstein, R., Longbottom, J., et al. (2021). Mapping underimmunized children in low- and middle-income countries. *Vaccine, 39*(27), 3665–3675.
37. Osgood-Zimmerman, A., Millear, A. I., Stubbs, R. W., et al. (2018). Mapping child growth failure in Africa between 2000 and 2015. *Nature, 555*(7694), 41–47.
38. Tatem, A. J., Weiss, D. J., Gibson, H. S., et al. (2021). Integrating geospatial data for health service accessibility and disease burden assessment. *International Journal of Health Geographics, 20*(1), 1–15.
39. Fullman, N., Yearwood, J., Abay, S. M., et al. (2018). Measuring performance on the Healthcare Access and Quality Index for 195 countries and territories. *The Lancet, 391*(10136), 2236–2271.
40. World Health Organization. (2023). Primary health care measurement framework and indicators. Geneva: WHO.
41. Cutter, S. L., Boruff, B. J., & Shirley, W. L. (2003). Social vulnerability to environmental hazards. *Social Science Quarterly, 84*(2), 242–261.

42. Flanagan, B. E., Gregory, E. W., Hallisey, E. J., et al. (2011). A social vulnerability index for disaster management. *Journal of Homeland Security and Emergency Management, 8*(1), 1–22.
43. World Health Organization. (2024). Integrated health services: Concepts, policy options and implementation strategies. Geneva: WHO.
44. UNICEF. (2024). Reaching zero-dose children through integrated service delivery approaches. New York: UNICEF.
45. Gavi, the Vaccine Alliance. (2024). The zero-dose learning agenda: Using data integration to identify underserved populations. Geneva: Gavi.